Single Event Effects Testing of the Linfinity SG1525A Pulse Width Modulator Controller

James. W. Howard Jr., *Senior Member, IEEE*, Martin. A. Carts, *Member, IEEE*,
Kenneth. A. LaBel, *Member, IEEE*, James. D. Forney and Timothy. L. Irwin

Abstract

The Linfinity SG1525A Pulse Width Modulator Controller was investigated for Single Event Effects. No latchup events were observed but pulse dropouts and multiple consecutive pulses were observed. Additionally, experimental data collection methodology led to erroneous temporal overlap events being observed. This methodology and care needed to avoid these effects will be discussed.

I.   Introduction

Pulse Width Modulator (PWM) Controllers are the heart of switching power supply systems in development today. The PWM Controllers considered here have the same integration advantages as many other controllers but they also include the drivers for the follow-on power Field Effect Transistors (FET). Previous work on these types of devices looked into the required test methodologies [1] and the impact of radiation on the soft start and shutdown circuits typically incorporated in the technology [2].

Taking advantage of this previous work this study was undertaken to determine the single event destructive and transient susceptibility of the Linfinity SG1525A Pulse Width Modulator Controller. The device was monitored for transient interruptions in the output signals and for destructive events induced by exposing it to a

heavy ion beam at the Texas A&M University Cyclotron Single Event Effects Test Facility and a laser beam at the Naval Research Laboratory Single Event Effects Test Facility. While exposing these devices to the beam, upset modes showing pulse dropouts and consecutive output pulses were observed. Initial testing also indicated a temporal overlap upset that was later shown to be a data collection anomaly.

The devices and the test methods used will be described first. This will be followed by a brief description of the data collected, the data collection anomaly, and a summary of the key results.

II.   Devices and Test Methods

SG1525A Devices

The SG1525A Pulse Width Modulator controller integrated circuit contains all logic and drivers required to implement all types of switching power supplies. It contains a 1% voltage reference, an oscillator with synchronization capability (to synchronize multiple devices), a pair of power FET drivers, programmable dead time control (to ensure one FET is off before the other begins to turn on), soft start circuitry, shutdown control, under-voltage shutdown, and a pulse latch-off circuit (to prevent any pulse, once terminated, from turning on again). The oscillator runs from 100 to 500 kHz. The device operates from 8 to 35 V_{dc} input, and the logic and the output drivers have independent supplies (V_{in} and V_c respectively). The DUT is designed for voltage feedback, modulating the width of each output pulse to maintain final filtered voltage stability. However, this application drives the outputs at maximum (50% duty cycle minus dead time of approximately 5%) with no feedback. Fig. 1 shows the functional block diagram of the SG1525A.

The device under test (DUT) was packaged in a 16-pin ceramic DIP. The DUTs tested were de-

lidded to allow the limited range ions and laser beam access to the active layer of the die.

Application and Test Hardware

The application for which these tests were conducted has two DUTs, termed the Master and Slave devices (See Fig. 2). They are synchronized together via the SYNC line out of the Master device and the Master device driven by an external 200 kHz reference frequency source (Normal mode). In the absence of the external frequency reference, the application circuit was designed to self-oscillate at some lower frequency, thus not losing total functionality (Free-run mode). The source voltage for both the DUT logic and the output driver collectors was 10.75 Volts (V_{dc}). Each DUT in the application circuit drives a pair of FETs, each at half the oscillator frequency, and each out of phase with the other. The FETs drive either end of a center-tap grounded transformer primary to ground when driven high (turned ON) by the DUT. The output of each DUT's transformer had multiple outputs, which were rectified and filtered.
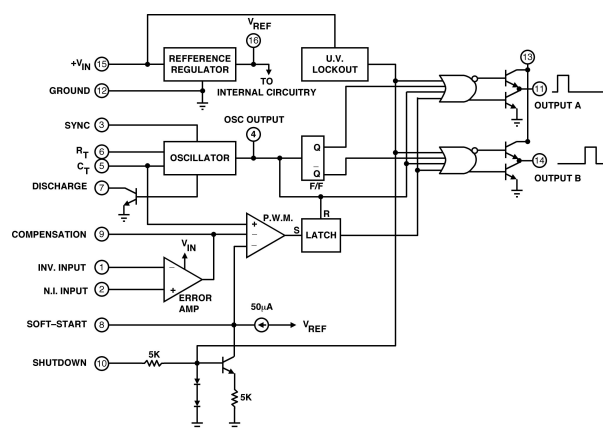

Fig. 1. Functional Block diagram of the SG1525A.

Reproducing the totality of this circuit, especially the FETs and transformer, was deemed cumbersome and of little value. Instead of trying to determine SEE from the filtered DC of the circuit's output, the DUT outputs were monitored, with simulated FET loading, for deviation from the nominal waveforms. Knowledge of the dynamics of the application circuit will allow the application circuit designers to determine the end effects of observed single events on the output voltages.

The application circuit's topology was reproduced for the DUTs, with some limitations and modifications (Fig. 2). The input voltage source was driven by an HP6626A power supply instead of a switching supply and the reference frequency input was supplied by a pulse generator. Also, the gates of the power FETs (and all following circuitry, transformers, rectifiers, filter capacitors) were simulated by an equivalent capacitance. The application FETs, 100V N channel enhancement mode radiation hardened FETs, have a C_{iss} (gate-source capacitance) of about 1000 pF, typically, and C_{rss} (gate-drain capacitance) of 45 pf. The Miller effect can magnify the effect of C_{rss}, but at a V_{ds} of only 10.75 Volts this did not have a significant effect in this case. The FET was simulated with a mica, 1100 pF capacitance to ground. The application circuit's 100 Ω series gate resistors were included in the test circuit.
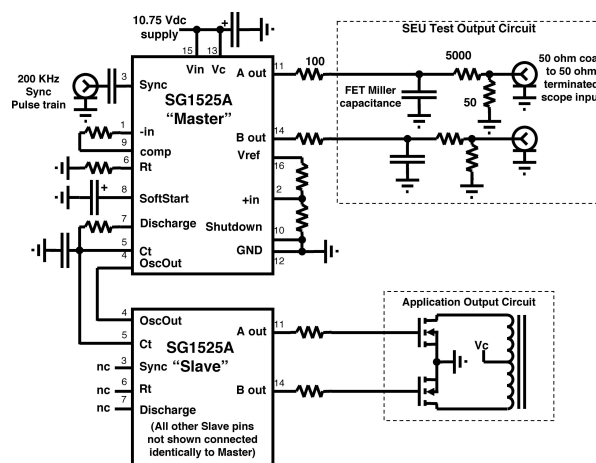

Fig. 2. Application and Test Circuit Diagram.

Two iterations of the two DUT circuit were built using good RF practices (specifically, ground plane and layout which minimized high frequency and power supply bypass capacitor trace lengths). Power and frequency reference were switched between circuits by relays. DUT outputs were not switched in order to maintain signal edge fidelity. Rather, all eight probe coaxial cables (two per DUT) were brought out of the irradiation area, so that switching from one DUT to another could be affected fairly rapidly. Relays were actuated by otherwise unused power supply outputs. Each DUT within a circuit was supplied

by a separate supply so that individual DUT currents could be monitored (See Fig. 3).

The DUT outputs were monitored directly at the DUT IC pins. Normally, low capacitance FET probes would be used to monitor signals with low loading effect, but in this case the 8 V linear range of the probes was too low to monitor the almost 11 V peak-to-peak signals. Instead, a high impedance high bandwidth probing technique was employed. A 5 kΩ resistor and a 50 Ω resistor (composed of a length of 50 Ω coax plus the scope's 50 Ω termination resistance on the far end) formed a resistive divider (amplitudes at the scope are reduced by approximately a factor of 100). The 5.05 kΩ load on the DUT pin was negligible. The bandwidth of the circuit was shown to be quite sufficient for these purposes. The coaxial cable and the oscilloscope's termination resistor are integral to the probe's operation, but the BNC connections were put there for ease of use. Also note that the output B signal was offset in voltage at the scope by approximately 10 mV, allowing for better monitoring of both output channels.
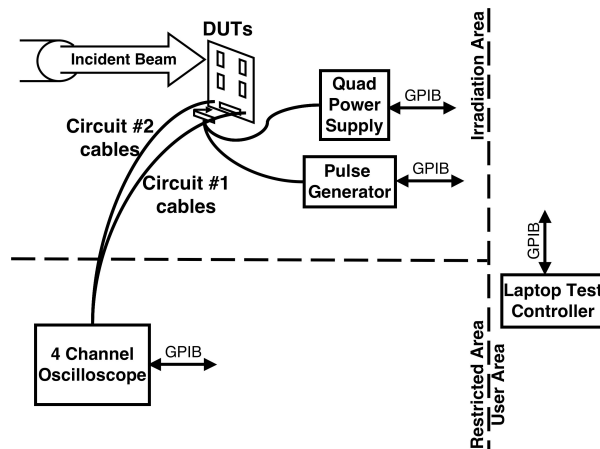

Fig. 3. Block diagram of the test setup.

Test Methodology

The SEE test process includes methods to test for all aspects of single event effects (latchup, functional interrupts, upsets, etc.). Individual DUT supply current has to be monitored to look for destructive failure modes and the output of the devices needs to be monitored while exercising the DUT to look for functional interrupts.

For these types of devices, there are many different effects that can be seen that could be interpreted as an upset, depending on how the device is used in a system. Therefore, in addition to monitoring the device output for an upset rate, the output may have to be monitored in various ways under the same test conditions using a different triggering scheme to collect data on the various types of upset mechanisms. To this end, data was collected using a number of triggering modes (described later) achieving a cross section measurement for each type of upset mode, as well as a total cross section (simply the sum of these individual rates).

The test flow for these devices included testing of both modes of operation (Normal (externally synchronized) and Free-run) and exposing each Master and Slave device to the ion beam. For these four test conditions, the output of either the Master or Slave device is monitored at the oscilloscope, leading to eight test conditions at each effective LET. DUT angles of 0, 30, 45, or 60 degrees were used to achieve an effective LET range from 8.6 to 61.3 MeV-cm^2/mg. This process was completed for two sets of devices, yielding the sample size of four. Finally, on one DUT at the higher normal incidence LET of 53.1 MeV-cm^2/mg, the V_{ds} was raised to 12 volts to perform an application worst-case latchup test.

Normal outputs from the SG1525A are shown in Fig. 4 for the two modes of operation (recall that the signal levels are 100X reduced and the channel B signal is offset for easier viewing). When exposed to the heavy ion beam, three primary modes of altering this output were originally observed. These were termed simple, double and overlap.

The triggering mode used to capture radiation-induced events was either Logic or Pulse mode. In Pulse mode, the scope will trigger when the time between pulses is greater than a given amount of time. This method will find error types that are either a shortening of one output pulse or the loss of a sequence of output pulses. If in Pulse mode, and the time is set to look for shorter gaps between pulses, then this triggering mode will find events that did not have the proper sequence of output A then B. This was the triggering method used during the initial testing.

In Logic mode, a triggering mode added for the laser and later heavy ion testing, the scope would trigger when the two inputs to the logic gate produce a true output. In this case, an AND

gate is used so that the scope will trigger when both signals are sufficiently high (> 20 mV).

For the test setup used here, Fig. 4 shows that the time between pulses under nominal operation is 6.2 µs for Normal mode and 86 µs for the Free-run mode. The actual widths for Pulse mode were set by varying the time (while the particle beam was off) until no trigger events were seen.
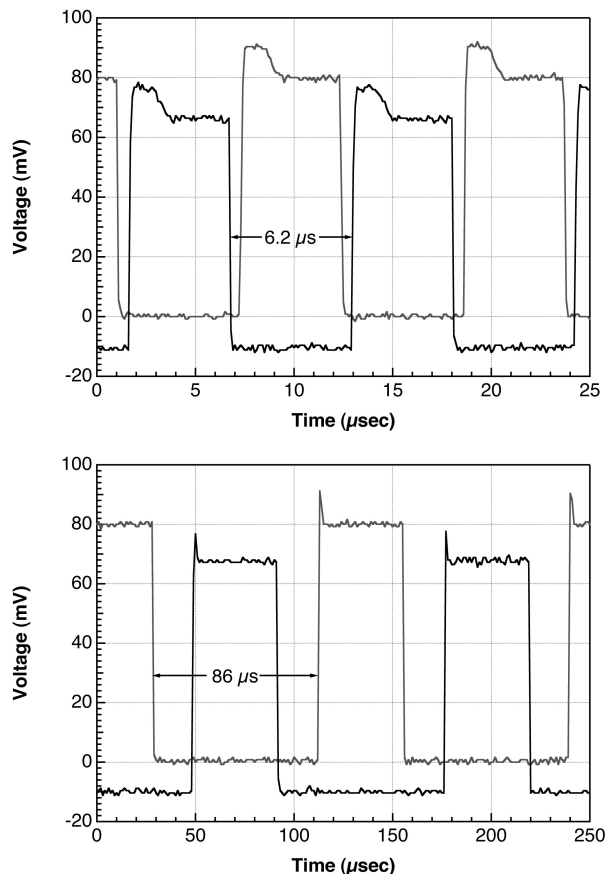

Fig. 4. Pre-rad traces for Normal (top) and Free-run (bottom) modes.

Test Facilities

These devices were tested at the Texas A&M University Cyclotron Single Event Effects Test Facility using 15 MeV/amu Argon, Krypton, and Xenon beams giving normal incident LETs from 8.6 to 53.1 MeV-cm^2/mg. The fluxes used ranged from 10^4 to 10^5 ions/cm^2/sec.

Additionally, the devices were exposed to a laser at the Naval Research Laboratory Single Event Effects Test Facility. The laser is a dye laser pumped by a Neodymium–doped Yttrium–Lithium–Fluoride (Nd:YLF) laser. The laser wavelength is 590 nm and energy of 3 pJ (energy

of the laser pulse could be varied with neutral density filters).

III. Results

Single Event Latchup

Four parts, biased at a nominal voltage of 10.75 V, were tested with heavy ions with LETs ranging from 8.6 to 61.3 MeV-cm^2/mg. Additionally, one part was exposed to an ion beam with an LET of 53.1 MeV-cm^2/mg while biased at 12 volts. These conditions were run while the devices were operated in both the Normal and Free-run modes. In no test condition were any high current conditions observed that would indicate any latchup or other destructive mode.

Initial Upset Testing Results

When exposed to the heavy ion irradiation during the initial testing, three primary modes of altering the nominal output were observed. These were termed simple, double and overlap (See Fig. 5).

A simple event is one in which the only observable difference is that one output pulse is either shortened or missing.

A double event is one where one of the outputs goes high consecutively, rather than alternating with the opposite output. It should be noted that the majority of the double events were seen on channel B. However, that is simply due to the triggering scheme used. There is no indication in the data sheet that would indicate either output having a preference for these double events.

The overlap event is one in which the two outputs lose their sync and the "highs" and "lows" overlap. This overlap condition existed from very short periods of time to complete overlap. The distribution of percent overlap was uniform, indicating no preference or mode in initiating this overlap condition.

Laser Testing

In an effort to understand the overlap events seen during the first test trip, the test setup was taken to the NRL Laser SEE Test Facility. At this facility, the top of the die was exposed to a focused laser beam to induce charge generation in the surface regions of the device. Using a photomicrograph of the die surface and a detailed circuit diagram obtained from the vendor, each

junction of each transistor of the device was sequentially exposed to laser light.
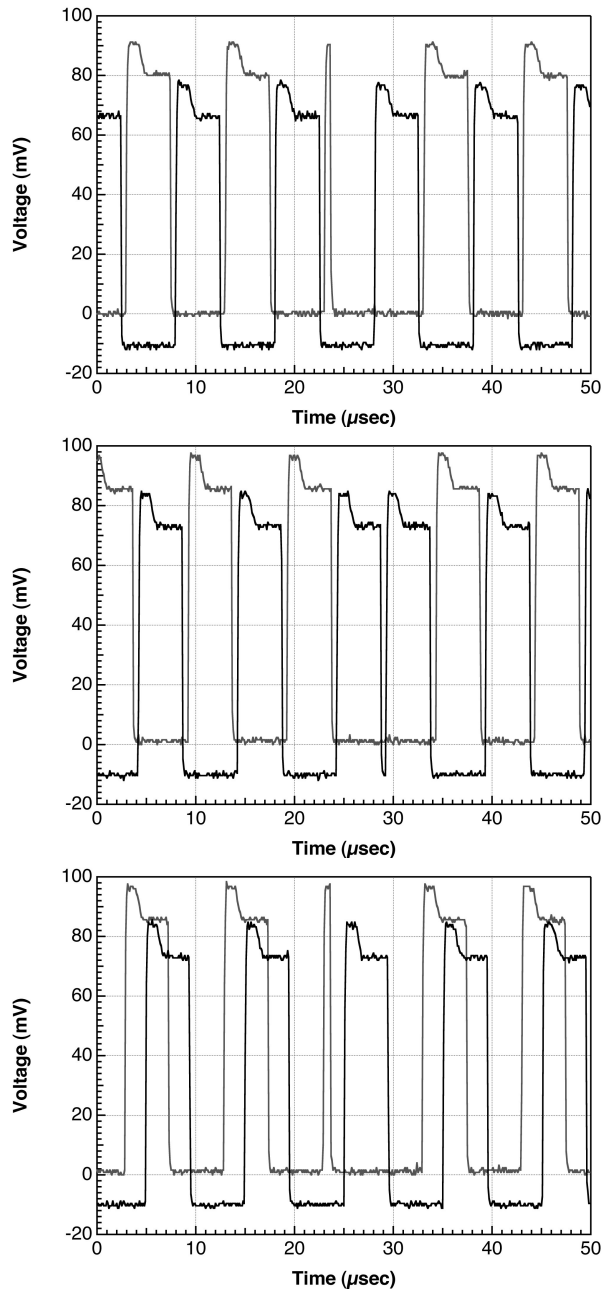

Fig. 5. Sample outputs showing simple (top), double (middle), and overlapping (bottom) events. Operation was in Normal mode and the LET was 8.6.

It is understood that the laser light cannot penetrate metal and has a finite range within the device. To deal with these limitations, both low intensity and high intensity beams were used, allowing, with high intensity beams, deeper penetration depths. Metallization was of little

concern for this device as it is very open, as can be seen in the photomicrograph shown in Fig. 6.

In addition to the change in source, the Logic triggering scheme was added (i.e., output pulse trains were observed, separately, with both Logic and Pulse triggering schemes in place). While utilizing the Pulse mode, a number of locations were noted across the die that would lead to either simple or double events. However, when the die was scanned using the Logic mode, no events were observed. This null result indicated that either the laser was not sufficiently penetrating into the sensitive area of the die to produce the effect, or there was some anomaly in the data collection mechanism during the first heavy ion test. In either case, a second heavy ion test was warranted.
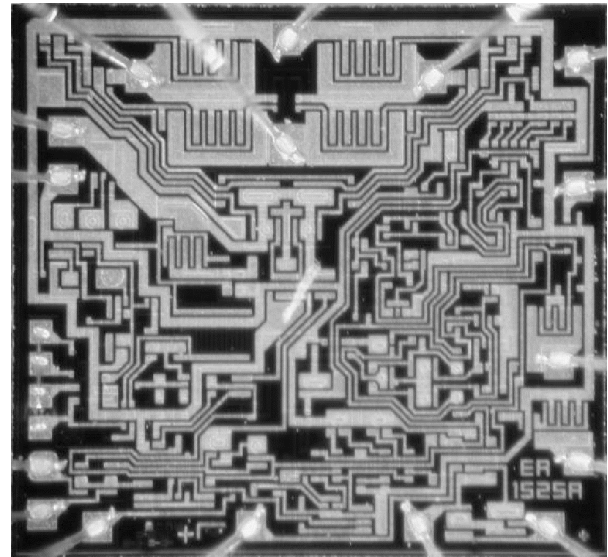

Fig. 6. Photomicrograph showing the SG1525A die metallization.

This second heavy ion test indicated a data collection anomaly was responsible for the overlap events. The cross section data for the device will be presented next – the data collection anomaly will be discussed later.

Single Event Upsets/Transients

In addition to the data collection with varying trigger schemes, data was collected with varying modes of operation (Normal and Free-run) and by what device was exposed (Master or Slave) and what device was monitored for errors (Master or Slave). This latter set of conditions was done to determine if errors generated in one device would

effect the proper operation of the other device. No transfer of error conditions was ever observed. Also, no variation was seen between the cases of exposing either the Master or Slave devices and monitoring that same device. Therefore, all cross section data presented here is for the Master/Master device combination.

Fig. 7 shows the upset cross section as a function of the effective LET for the two modes of operation. In each graph of Fig. 7, the cross section for double events and the total cross section (sum of simple and double events) are plotted, along with the respective Weibull fits to the experimental data points. As can be seen in these graphs, the double events occur at a rate of one in five to one in ten as compared to the total cross section, independent of which mode the device was operated. In the case of Normal mode, though, the saturation cross section is much flatter (and lower in value) and has a lower threshold LET than the Free-run mode.

Fig. 8 shows the same cross section data but now plotted as a function of event type and comparing modes of operation with the graphs.

In the top graph of Fig. 8, where all events are considered, the data is consistent across both modes of operation and one Weibull fit can adequately describe both data sets. The Weibull fit for these data sets yields a threshold LET of approximately 5 MeV-cm^2/mg and a saturation cross section of approximately 2×10^{-4} cm^2.

In the lower graph of Fig. 8, the double event cross sections are plotted for the two modes of operation. When plotted in this manner, the differences between the two modes of operation, mentioned above, become obvious. The threshold LET is about a factor of two higher for the Normal mode of operation and its saturation cross section is a factor of 3 to 4 higher, as well. It should be mentioned, however, that the statistics (number of observed double events) for the Free-run mode was limited in the low LETs, making an accurate determination of threshold problematic.

IV.   Discussion

This paper was originally submitted to discuss the possibly catastrophic events that were observed in the initial testing. In this test, events were observed that had the two outputs having high levels for some period of time. If this condition existed, the two power MOSFETs of the

application circuit would have been turned on for this period, providing a low resistance path from the power supply to ground. If the overlap time was sufficient, this could have led to destructive events.
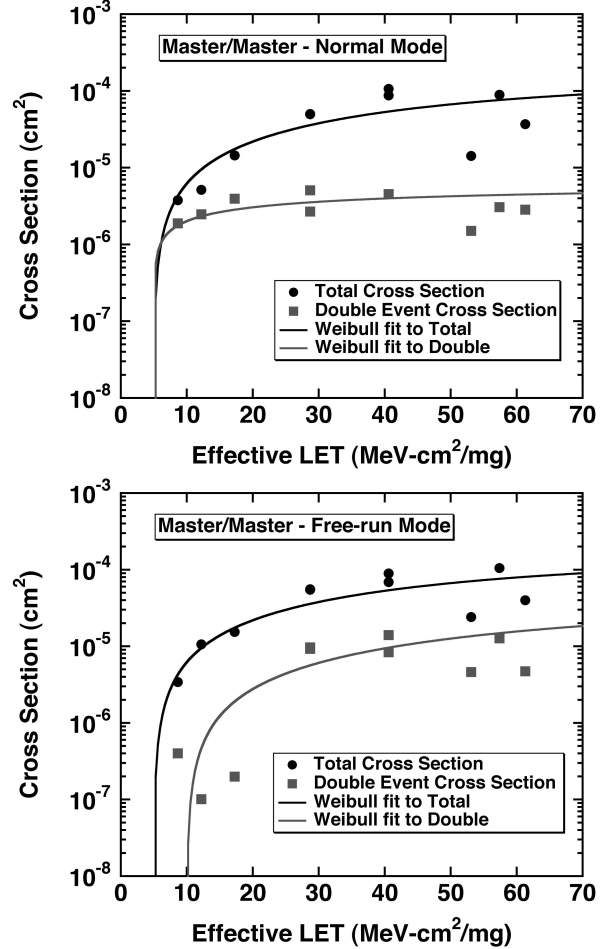

Fig. 7. Cross section curves for Normal (top) and Free-run (bottom) modes for both total and double events as a function of Effective LET.

The vendor was contacted and detailed circuit diagrams were obtained. Die photomicrographs were taken and the devices were taken to the laser facility, as described previously. When the laser did not demonstrate the overlap events, the suspicion was raised that the data collection method could be at fault. At issue, though, was the fact that this data collection methodology had been successfully used many times in the past. Some in-laboratory testing did indicate that there could be some problems that involved using the digital scope with two independent channels of data processed through software into the data

collection computer (possibly through the use of the complex triggering schemes used).
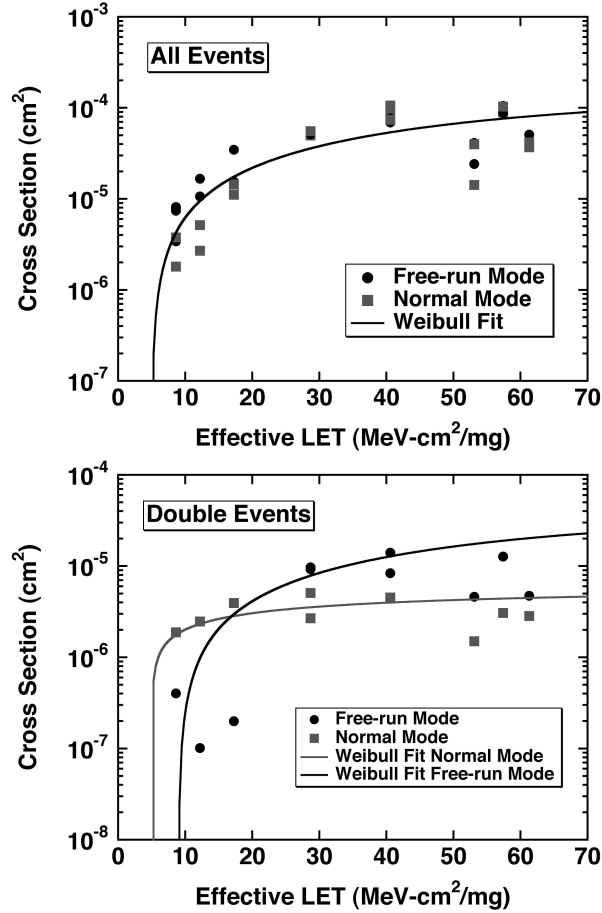

Fig. 8. Cross section curves for All Events (top) and Double Events (bottom) for both Normal and Free-run modes as a function of Effective LET.

It did turn out that this was indeed the case. Our normal data collection methodology allowed for the collection of the count of all events occurring as the parts were exposed and the collection of the digital signature of a portion of the total events. While this had been done numerous times in the past, this was the first case where the digital signature of the event had two independent signals. The crux of the problem stems from the fact that the digital scope in question does not have a command to download all active channels. Each active channel must be downloaded in sequence. There is a window from the time the data has begun downloading for the first channel and the computer gives the command for the second channel to be downloaded. During this window, the scope allows trigger events. We

always maintained a low event rate, however, due to the probabilistic nature of the events, there were cases where an event triggered the scope in between channel downloads, leading to the case where channel 1 data was from event *n* and channel 2 data was from event *n+1*. If the trigger point was not at exactly the same time (as was typically the case where the primary event is pulse shortening), the time bases would be skewed and an apparent overlap event would be registered.

To verify this, the triggering of the scope was changed to Single-Shot mode. In this mode, once a trigger event would occur, the scope would not re-arm for another trigger until the computer sent a command to do so. This allowed for both channels of data to be downloaded to the computer before the command was sent to re-arm the trigger. The disadvantage of this methodology is two-fold. First, the data collection rate is substantially reduced. Secondly, with the scope sitting idle for a significant percentage of the time, no accurate measure of the total number of events can be obtained at the same time as the event signatures.

When this Single-Shot mode was used, independent of what method was used to initiate the triggering, no overlap events were ever observed. This observation led to the conclusion that no real overlap events were observed in the initial testing and these overlap events were just artifacts of the collection methodology. The oscilloscope captures with this artificial overlap condition were triggered by some other event, either a simple or double event. The first data set was then re-analyzed with this in mind and the appropriate cross sections calculated accordingly. This is the data set reported in this paper.

V.   Summary

This paper reports on the heavy ion Single Events Effects testing of the Linfinity SG1525A Pulse Width Modulator Controller. The results have shown no catastrophic failure modes. The initial testing did show an event that could lead to a catastrophic event. However, additional testing with a laser system and heavy ions indicated that these events were simply an anomaly created by the data collection methodology.

The true events for this device were simple and double events that lasted for no more than one clock cycle. Most power supply systems that

would use a PWM, such as the SG1525A, would not be affected by these minor events. Therefore, these devices would be considered acceptable for use in space flight systems.

VI.   References

[1] S.H.Penzin,   W.R.Crain,   K.B.Crawford, S.J.Hansel and R.Koga, "The SEU in Pulse Width Modulator Controllers with Soft Start and Shutdown Circuits", 1997 IEEE Radiation Effects Data Workshop Record.

[2] S.H.Penzin,   W.R.Crain,   K.B.Crawford, S.J.Hansel, J.F.Kirshman and R.Koga, "Single Event Effects in Pulse Modulation Controllers", IEEE Transactions on Nuclear Science, Vol. 43, No. 6, December 1996.

[3] H.W.Johnson and M.Graham, *High Speed Digital Design, a Handbook of Black Magic*, Section 3.5, Prentice Hall PTR, 1993.